R. CHMIELOWSKI*, **, V. MADIGOU*, M. A. FRÉMY*, M. BLICHARSKI**, G. NIHOUL*

STRUCTURAL ANALYSIS OF $Sr_{n+1}Ru_nO_{3n+1}$ THIN FILMS DEPOSITED BY LASER ABLATION

ANALIZA STRUKTURY CIENKICH WARSTW $Sr_{n+1}Ru_nO_{3n+1}$ OTRZYMANYCH TECHNIKĄ ABLACJI LASEROWEJ

The series of conductive oxides, $Sr_{n+1}Ru_nO_{3n+1}$, has been studied for applications in microelectronics as these oxides could be interesting electrode materials for ferroelectric memories (FeRAM). Sr_2RuO_4 seems to be an interesting candidate. Thin films of Sr_2RuO_4 were obtained by pulsed laser deposition on a Si (001) substrate. The influence of deposition times and pulse frequencies on the microstructure and properties of the deposited thin films was analysed. Thin films characterization was done by X-ray diffraction, EDS microanalysis, scanning electron microscopy, high-resolution transmission electron microscopy and conductivity measurements. Most of the films are composed of several oxides of the $Sr_{n+1}Ru_nO_{3n+1}$ series. However, their surface is well-defined and, for some films, the conductivity is interesting for applications. Deposition parameters have strong influence on composition and microstructure of oxides films.

Keywords: Strontium ruthenate, FeRAM, Pulsed Laser Deposition

Badania struktury krystalicznej, mikrostruktury oraz własności elektrycznych cienkich warstw, które mają mieć zastosowanie jako elektrody w pamięciach ferroelektrycznych (FeRAM) skupiają się na materiałach tlenkowych. Jednym z nich jest Sr_2RuO_4 należący do grupy tlenków $Sr_{n+1}Ru_nO_{3n+1}$, charakteryzujących się dobrymi własnościami elektrycznymi. Cienkie warstwy z Sr_2RuO_4 osadzono techniką ablacji laserowej na płaszczyźnie (001) monokryształu krzemu. Analizowano wpływ czasu ekspozycji oraz częstotliwości impulsów laserowych na strukturę i własności otrzymanych warstw. Badania prowadzono z wykorzystaniem, rentgenowskiej dyfrakcyjnej analizy fazowej, mikroanalizatora EDS oraz za pomocą skaningowej mikroskopii elektronowej i transmisyjnej mikroskopii elektronowej. Przeprowadzone badania własności elektrycznych wykazały przydatność cienkich warstw do zastosowań na elektrody w układach mikroelektronicznych.

1. Introduction

It has been shown that elaboration of ferroelectric memories (FeRAM), with conductive oxide as an electrode could prevent ageing by supplying oxygen to the interface with the dielectric [1, 2]. The best candidates for the ferroelectric materials are members of the Aurivillius series, $Bi_2A_{n-1}B_nO_{3n+3}$ [3]. Several of the members of the Ruddlesden-Popper (RP) series, $Sr_{n+1}Ru_nO_{3n+1}$, are conductive and could lead to a good epitaxy with the Aurivillius series [4]. Hence, the goal of the paper is to investigate the possibility of using RP oxides as a substrate when elaborating Aurivillius FeRAM. $SrRuO_3$ (n = ∞ in Ruddlesden-Popper series) has already been tried, but doesn't present epitaxial relations with the Aurivillius phase. So, we have chosen Sr_2RuO_4 (n = 1) which provides interesting possibilities of epitaxy [5]. It has a K_2NiF_4 crystal structure [6, 7] and shows high metallic conductivity along the a-b plane (10^{-4} $\Omega\cdot$cm at room temperature) [7, 8]. It is expected that investigation of Sr_2RuO_4 thin films would lead to new electrode materials for microelectronic applications. In this work some structural analyses of the thin films deposited by Pulsed Laser Deposition (PLD) were done. The PLD method was chosen because it produces highly excited particles which high kinetic energy can provide crystal growth at relatively low temperatures. In our case, to prevent silicon diffusion, the substrate temperature cannot be higher than 700°C.

2. Experimental

The Sr_2RuO_4 target for PLD was prepared by the solid state reaction $SrCO_3 + RuO_2 => Sr_2RuO_4 + CO_2$.

* LABORATORY OF MATERIALS MICROELECTRONICS OF PROVENCE, CNRS-UMR 6137, UNIVERSITY DU SUD TOULON-VAR, BP20132, 83957 LA GARDE CEDEX, FRANCE
** AGH UNIVERSITY OF SCIENCE AND TECHNOLOGY, FACULTY OF METALS ENGINEERING AND INDUSTRIAL COMPUTER SCIENCE, 30-059 KRAKÓW, AL. MICKIEWICZA 30, POLAND

First, the $SrCO_3$ and RuO_2 powders were mixed in an agate mortar. The proportions of $SrCO_3$ and RuO_2 were not stoichiometric because it was found that an addition of RuO_2 in excess 2.5 at.% leads to the best final composition of the Sr_2RuO_4 target. The mixed powders were compacted and heated at temperature 1150°C for 24 h, then ground again, recompacted and heated at temperature 1200°C for 36 h. The target final diameter and thickness were 30 mm and 2.5 mm, respectively.

$Sr_{n+1}Ru_nO_{3n+1}$ thin films were deposited on a Si (001) substrate by an excimer laser (system Compex 301 of Lambda Physics), working with the following process parameters: wavelength 248 nm (KrF radiation), energy density on the target 1.5 J · cm^{-2}, pulse duration 30 ns, fixed laser beam size of 2×5 mm^2 and target substrate distance 60 mm. The laser beam hits the target at an incidence angle 45°. Target and silicon substrate were parallel, the oxygen partial pressure was 40 Pa and the substrate temperature 600°C. Two frequencies 2 and 6 Hz of the laser impulse were used. Three deposition times, corresponding to 1000, 2000, 4000 laser impulses were tried. This leads to different thicknesses of the deposited films. The samples are noted SRXY, where X indicated the frequency of the laser (2 or 6 Hz) and Y the thousand of laser impulses (1, 2, or 4). Deposition conditions are summarized in Table.

TABLE

Parameters of the deposition conditions and deposited thin films: frequency ω, number of impulses n, size of the agglomerated grain l, thickness d, phases identified by X-ray diffraction, resistivity ρ, (P_{O_2} = 40 Pa , T = 600°C)

Sample	ω, Hz	n	l, nm	d, nm	Probable phases, XRD	$\rho, \Omega \cdot$cm
SR21	2	1000	58 ± 9	50 ± 6	$SrRuO_3$, some Sr_2RuO_4 and $Sr_3Ru_2O_7$	0.5
SR22	2	2000	70 ± 13	75 ± 13	$Sr_3Ru_2O_7$, some Sr_2RuO_4 and $SrRuO_3$	430
SR24	2	4000	76 ± 13	114 ± 10	Sr_2RuO_4, $Sr_3Ru_2O_7$, some $SrRuO_3$	770
SR61	6	1000	50 ± 13	26 ± 3	Sr_2RuO_4, $Sr_3Ru_2O_7$, some $SrRuO_3$	1.9
SR62	6	2000	56 ± 13	33 ± 10	Sr_2RuO_4, $Sr_3Ru_2O_7$, few $SrRuO_3$	13.6
SR64	6	4000	63 ± 13	95 ± 9	Sr_2RuO_4, some $Sr_3Ru_2O_7$ and $SrRuO_3$	15.8

The influence of the deposition parameters on the microstructure, composition and properties of the deposited thin films was analysed. Samples were characterized by X-ray diffraction (XRD) on a Siemens D5000 diffractometer, scanning electron microscopy (SEM) on a Jeol JSM-6320F and transmission electron microscopy (TEM) on a FEI Technaï G^2, both coupled with an energy dispersive spectrometer (EDS). Conductivity measurements were performed by the 4-points method, on a laboratory device coupled with a digital multimeter HP34401A.

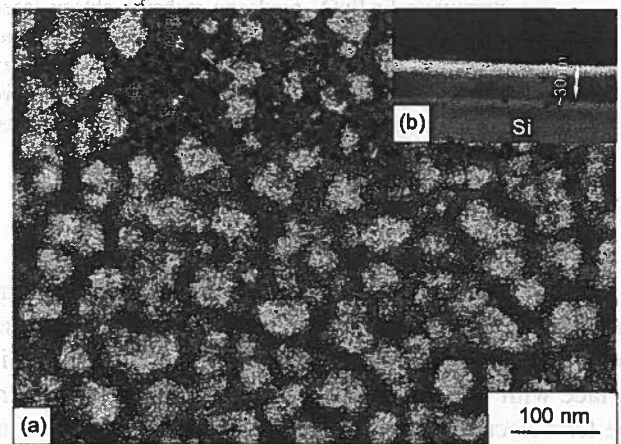

Fig. 1. SEM micrographs of SR21 thin film (a) surface image; (b) cross-section

3. Results and discussion

The film thicknesses and the average size of agglomerated grains, measured on the SEM micrographs for different deposition conditions are given in Table. As expected, the film thickness increases with the deposition time but the relation between them is not linear. However, this behaviour could be due to a non constant wear of the target during the ablation process; it was observed in both series of samples, SR2Y and SR6Y.

Two characteristic samples (SR21 and SR64) have been chosen to show microstructures of the thin films. Plane views and cross-sections of these samples are exhibited on Fig. 1 and 2. The samples which were elaborated with a 2 Hz laser frequency (SR2Y) show microstructures with a larger average size of the agglomerated grains and the films are thicker than for respective films which were deposited with a 6 Hz laser frequency. All films have good smooth surfaces. In general, the elements of the microstructure of thicker film, are sharper and more compact than in the case of thinner films. The same relations are observed for SR2Y and SR6Y series.

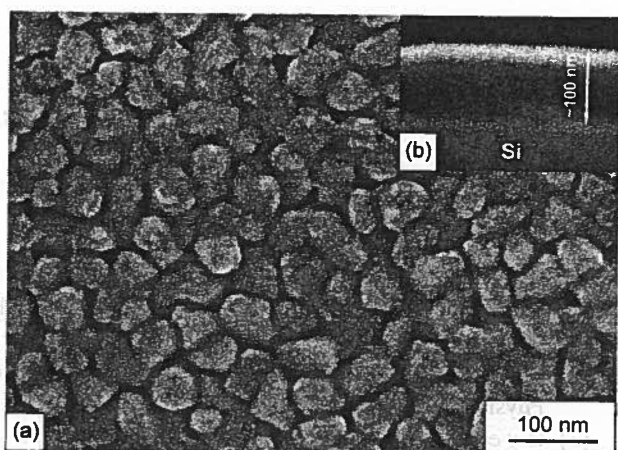

Fig. 2. SEM micrographs of SR64 thin film (a) surface image; (b) cross-section

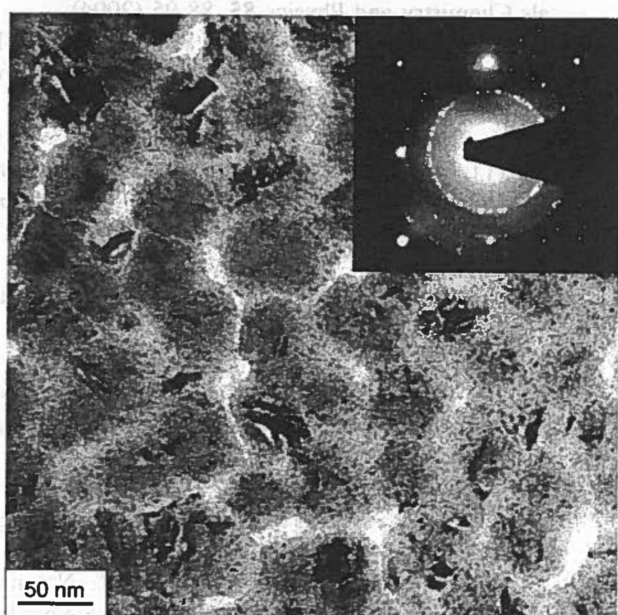

Fig. 3. TEM micrograph and diffraction pattern of the plane view SR61, the intense spots correspond to silicon, while the rings correspond to Sr_2RuO_4 and $SrRuO_3$

The microstructure of the SR61 sample imaged by transmission electron microscopy in planar view in normal resolution (Fig. 3) is very similar to the microstructure imaged by SEM (Fig. 1 and 2), but the dotted rings in the diffraction pattern indicate that the diffracting domains are in fact smaller than illustrated by SEM elements of microstructure. This is confirmed by the HREM, where in the cross-section view small crystallites (2 to 3 nm) are present (Fig. 4). These crystallites tend to agglomerate to form the larger particles observed on SEM and TEM. From the Fourier transforms performed on the HREM images, the measurement of interplanar distances is possible but it is very difficult to identify the phases because some values could correspond to several phases ($SrRuO_3$, Sr_2RuO_4, $Sr_3Ru_2O_7$, $Sr_4Ru_2O_9$). However, analyses indicate that several phases are present (see also the diffraction pattern on figure 3). The XRD patterns (Fig. 5) are difficult to interpret because only one peak coming from the layer can be seen. Even this peak, which corresponds to the main peak for all structures, is broadened and has a weak intensity. The first problem is explained by the small (2 to 3 nm) size of the crystallites measured on the HREM image (Fig. 4). The second problem is due to the small thickness of the film, specially for samples SR61 and SR62. All the phases $SrRuO_3$, Sr_2RuO_4, $Sr_3Ru_2O_7$ and $Sr_4Ru_2O_9$ have their strong diffraction peaks near the same 2θ value. However, from these XRD spectra, a qualitative information can be obtained and this is given in Table. The EDS analysis coupled to the microscopic observations give different results for the different samples ranging from 65 at.% Sr and 35 at.% Ru, to 58 at.% Sr and 42 at.% Ru.

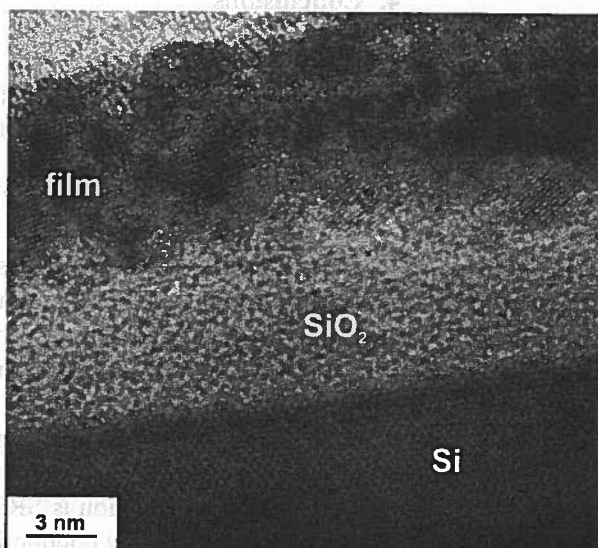

Fig. 4. HREM micrograph of the cross-section SR61

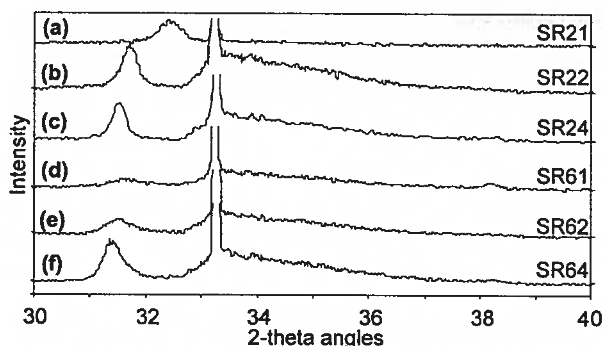

Fig. 5. X-ray diffraction pattern of the thin films

Bulk samples of Sr_2RuO_4 have conductivity about $10^{-4}\ \Omega \cdot cm$. Thin films, with many grain boundaries are

bound to have a higher resistivity. In our case no film has a resistivity low enough to be attributed to Sr_2RuO_4. The conductivity results vary in concordance with the XRD results and are shown in Table. The best conductivity is presented in SR21 but it is probably due by the predominant phase of the conductive oxide $SrRuO_3$ which has isotropic conductive properties.

Only few studies have been made on the relative stability of the different members of the RP series. A schematic phase diagram has been proposed [9]. Some authors using very high substrate temperatures and very low oxygen partial pressures during the PLD process have obtained pure Sr_2RuO_4 [10]. In our case Sr_2RuO_4 is not the most stable component, but some results can be already summarized.

4. Conclusions

- Thin films deposited by PLD are composed of grains whose sizes are about 2-3 nm which form agglomerates about fifteen times larger.
- Films are composed of several oxides of the $Sr_{n+1}Ru_nO_{3n+1}$ series.
- Thin films of the series deposited with higher laser frequency are more compact, thinner and they have smaller size of agglomerated grains than the thin films of the series deposited in lower laser frequency.
- The conductivity of the samples deposited with higher laser frequency is better than the samples deposited with lower laser frequency (an exception is SR21, where the predominant phase is probably conductive oxide $SrRuO_3$).

Received: 5 January 2006.

Acknowledgements

This work was financially supported by the Polish Ministry of Education and Science through the project no 3T08A 080 28.

REFERENCES

[1] A. M. Dhote, S. Madhukar, W. Wei, T. Venkatesan, R. Ramesh, C. M. Cotell, Applied Physics Letters **68**, 1350-1352 (1996).

[2] K. S. Liu, T. F. Tseng, I. N. Lin, Applied Physics Letters **72**, 1182-1184 (1998).

[3] Hye In Kim, Young Soo Sog, Sok J., Chee Won Chung, Thin Solid Films **429**, 114-118 (2003).

[4] Ta-Jeng Wu, Dah-Shyang Tsai, Materials Chemistry and Physics **85**, 88-95 (2004).

[5] S. Léonard, S. Villain, V. Madigou, E. Nigrelli, C. Cesari, G. Nihoul, Ferroelectrics **288**, 1-9 (2003).

[6] M. K. Crawford, R. L. Harlow, W. Marshall, Z. Li, G. Cao, R. L. Lindstrom, Q. Huang, J. W. Lynn, Physical Review B **65**, 214412 (2002).

[7] F. Lichtenberg, A. Catana, J. Mannhart, D. G. Schlom, Applied Physics Letters **60**, 1138-1140 (1992).

[8] D. Reyes Ardila, M. R. B. Andreeta, S. L. Cuffini, A. C. Hernandes, J. P. Andreeta, Y. P. Mascarenhas, Journal of Crystal Growth **177**, 52-56 (1997).

[9] K. Thomas Jacob, Kay Thi Lwin, Yoshio Waseda, Materials Science and Engineering **B103**, 152-161 (2003).

[10] S. Madhavan, J. A. Mitchell, T. Nemoto, S. Wozniak, Ying Liu, D. G. Scholm, A. Dabkowski, H. A. Dabkowska, J. Crys. Growth **174**, 417-423 (1997).